

Simplified seismic analysis procedures for elevated tanks considering fluid–structure–soil interaction

R. Livaoğlu^{a,*}, A. Doğangün^b

^a*Department of Civil Engineering, Karadeniz Technical University, 29000 Gumushane, Turkey*

^b*Department of Civil Engineering, Karadeniz Technical University, 61080 Trabzon, Turkey*

Received 25 May 2005; accepted 27 December 2005

Available online 28 February 2006

Abstract

This paper presents a review of simplified seismic design procedures for elevated tanks and the applicability of general-purpose structural analyses programs to fluid–structure–soil interaction problems for these kinds of tanks. Ten models are evaluated by using mechanical and finite-element modelling techniques. An added mass approach for the fluid–structure interaction, and the massless foundation and substructure approaches for the soil–structure interactions are presented. The applicability of these ten models for the seismic design of the elevated tanks with four different subsoil classes are emphasized and illustrated. Designers may use the models presented in this study without using any fluid and/or special soil elements. From the models defined here, single lumped-mass models underestimate the base shear and the overturning moment. Because almost all the other assumptions for the fixed base give similar results, any method could be used, but the distributed added mass with the sloshing mass is more appropriate than the lumped mass assumptions for finite-element modelling, and is recommended in this study.

© 2006 Elsevier Ltd. All rights reserved.

Keywords: Elevated tanks; Fluid–structure interaction; Soil structure interaction; Simplified procedures

1. Introduction

Water supply is essential for controlling fires that may occur during earthquakes, which cause a great deal of damage and loss of lives. Therefore, elevated tanks should remain functional in the post-earthquake period to ensure water supply is available in earthquake-affected regions. Nevertheless, several elevated tanks were damaged or collapsed during past earthquakes (Haroun and Ellaithy, 1985; Rai, 2002). Therefore, the seismic behavior of elevated tanks should be known and understood, and they should be designed to be earthquake-resistant. Comparisons of the studies about this subject with those of the ground-supported cylindrical tanks is difficult, however, as few studies have been carried out related to the seismic behavior of elevated tanks.

Due to the fluid–structure–soil/foundation interactions, the seismic behavior of elevated tanks has the characteristics of complex phenomena. Tens of studies have been carried out and many special programs have been coded to analyze the fluid–structure and/or the soil–structure interactions for other liquid storage structures, such as ground-supported cylindrical tanks (Fischer et al., 1991; Zeiny, 1995) and dams (Chavez and Fenves, 1994; Tan and Chopra, 1996). Some

*Corresponding author. Tel.: +90 456 2337425; fax: +90 456 2337427.

E-mail addresses: rлива@ktu.edu.tr (R. Livaoğlu), adem@ktu.edu.tr (A. Doğangün).

general programs have been carried out, which cover large amounts of data; these programs include ADINA (2004), ANSYS (2004) and SOLVIA (2004). Although many large companies have participated in these programs, it is difficult for most designers to obtain the required special programs that cover a large amount of data in many countries. However, a general-purpose structural analysis program generally exists in every engineering office. So, the evaluation of the applicability of these structural analysis programs in the design of elevated tanks is important from an engineering point of view and it will be helpful to present the application and results to designers. There is a second important reason that should be considered. That is, simplified models are used for a straightforward estimate of the seismic hazard of existing elevated tanks. Only if the estimated risk is high, it is convenient to measure all the data (e.g. geometry of the tank, material properties) that are required by the general finite element codes and to spend time and money to prepare a reliable general model. Moreover, as in the past, simple engineering approximations will be developed in the future.

Finally, two main purposes have been selected for this paper. One of them is to evaluate simplified models for elevated tanks that have been developed by different researchers and recommended by current major earthquake codes. The other is to investigate the applicability of the finite-element models using general-purpose structural analysis programs for fluid–structure–soil interaction problems for elevated tanks and to present the results to designers.

2. Single lumped-mass model

The concept that enables analysis of elevated water tanks as a single lumped-mass model was suggested in the 1950s (Chandrasekaran and Krishna, 1954). Elevated tanks (Fig. 1) and the selected model for this concept can be seen in Fig. 1(e). Two significant points should be discussed for this concept. The first point is related to the behavior of the fluid. If the container is completely full of water, this prevents the vertical motion of water sloshing, so the elevated tank may be treated as a single-degree-of-freedom system in such a case. When the fluid in the container (vessel) oscillates, this concept fails to characterize the real behavior. The other point is related to the supporting structures. As the ductility and the energy-absorbing capacities are mainly regulated by the supporting structure, this is important for the seismic design of elevated tanks. In this model, it is assumed that the supporting structure has a uniform rigidity along the height. The elevated tanks can have different types of supporting structures, which could be in the form of a steel frame, a reinforced concrete shell, a reinforced concrete frame or a masonry pedestal. Under seismic loads, the supporting structures that act as a cantilever of uniform rigidity along the height cannot represent all the supporting structure types. But it may be that these are more suitable for the reinforced concrete shell supporting structure, as shown in Fig. 1(a).

The Indian seismic code, IS:1893, requires elevated tanks to be analyzed as a single-degree-of-freedom system—that is, a one-mass system—which suggests that all fluid mass participates in the impulsive mode of vibration and moves with the container wall (Rai, 2002). It must be stated that this can be a realistic assumption for long and slender tank containers with a height-to-radius ratio exceeding four. Also, the ACI 371R-98 (1995) suggests that the single lumped-mass model should be used when the water load (W_w) is 80% or more of the total gravity load (W_G) that includes: the total dead load above the base, water load and a minimum of 25% of the floor live load in areas that are used for storage. For this model, the lateral flexural stiffness of the supporting structure (k_s) is determined by the deflection of

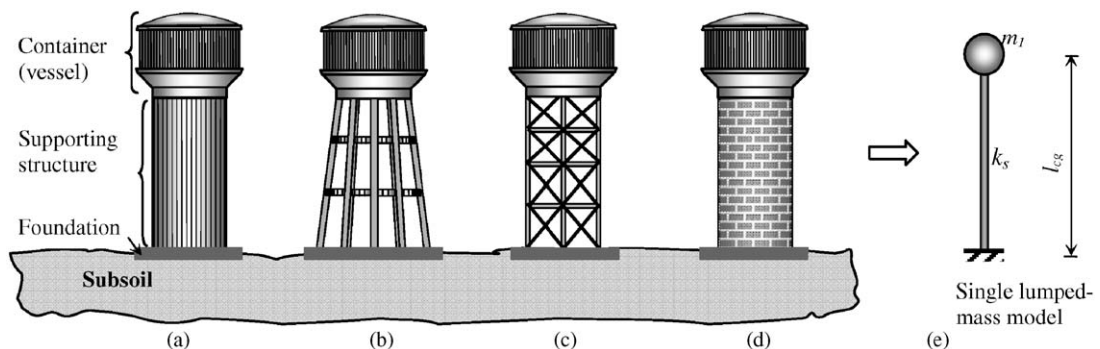


Fig. 1. Elevated tanks and the single lumped-mass model: (a) the tank with reinforced concrete shaft supporting structure, (b) the tank with reinforced concrete frame supporting structure, (c) the tank with reinforced concrete frame with diagonal braces or steel frame supporting structure, (d) the tank with masonry pedestal supporting structure, (e) single lumped-mass model.

the concrete supporting structure acting as a cantilever beam,

$$k_s = \frac{3EI_c}{l_{cg}^3}, \tag{1}$$

where l_{cg} is the distance from the base to the centroid of the stored water, E the Young’s modulus of the material and I_c the moment of inertia of the gross section about centroidal axis neglecting reinforcement.

The fundamental period of the vibration T of the elevated tanks should be established by

$$T = 2\pi\sqrt{\frac{W_L}{gk_s}} \tag{2}$$

according to ACI 371R, where g is the ground acceleration, W_L is the single lumped-mass structure weight consisting of (a) self-weight of the container, (b) maximum of two-thirds (66%) the self-weight of the concrete support wall, and (c) the water weight.

After the calculation of the period and the selection of the damping value, the base shear and overturning moments can be estimated from the standard response spectrum analyses.

3. Approaches for modelling the fluid–structure system

Mechanical models based on analytical methods and some finite-element approximations by taking the effect of the fluid into account are presented below.

3.1. Simplified models

The equivalent spring-mass models have been proposed by some researchers to consider the dynamic behavior of the fluid inside a container as shown in Fig. 2. The fluid is replaced by an impulsive mass m_i that is rigidly attached to the tank container wall and by the convective masses m_{cn} that are connected to the walls through the springs of stiffness (k_{cn}). According to the literature, although only the first convective mass may be considered (Housner, 1963), additional higher-mode convective masses may also be included (Chen and Barber, 1976; Bauer, 1964) for the ground-supported tanks. A single convective mass is generally used for the practical design of the elevated tanks (Haroun and Housner, 1981; Livaoğlu and Doğangün, 2005) and higher modes of sloshing have negligible influence on the forces exerted on the container even if the fundamental frequency of the structure is in the vicinity of one of the natural frequencies of sloshing (Haroun and Ellaithy, 1985). As practical analyses are presented in this study, only one convective mass is taken into consideration in the numerical examples. Haroun and Housner (1981) have also developed a three-mass model of ground-supported tanks that takes tank-wall flexibility into account. Here, as the elevated tanks are considered to be reinforced concrete, the flexibility of the walls is ignored and the third-mass is not considered for the simplified models that were used in this paper.

A simplified analysis procedure has been suggested by Housner (1963) for fixed-base elevated tanks (Fig. 3). In this approach, the two masses (m_1 and m_2) are assumed to be uncoupled and the earthquake forces on the support are estimated by considering two separate single-degree-of-freedom systems: The mass of m_2 represents only the sloshing of

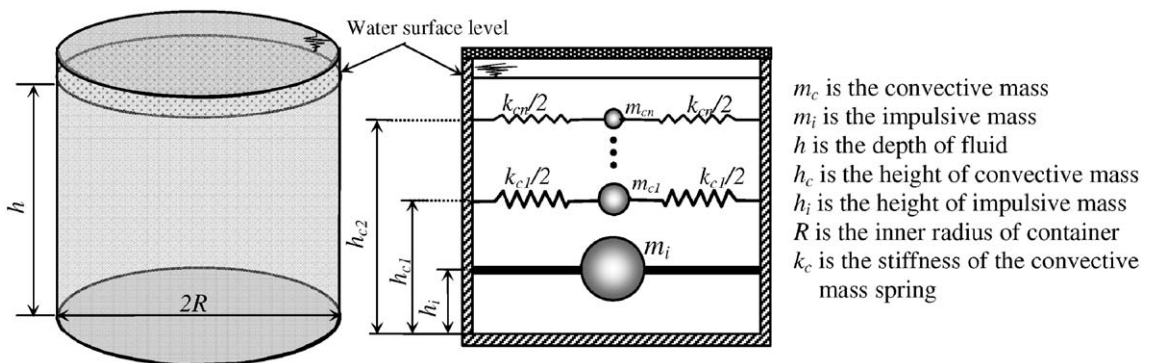


Fig. 2. Spring-mass analogy for ground supported cylindrical tanks.

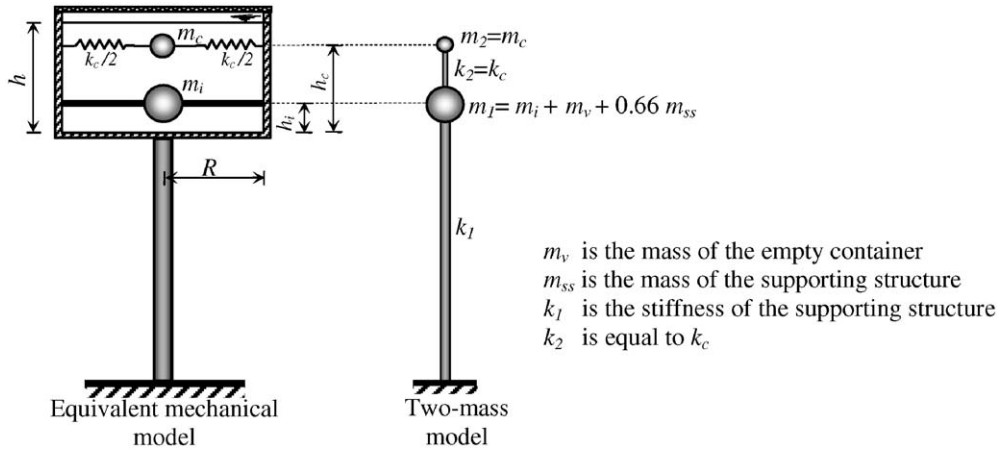


Fig. 3. Two-mass model for the elevated tanks suggested by Housner.

Table 1
Parameters for the spring-mass analogy recommended by Housner and Bauer

Description	Bauer's model (Chen and Barber, 1976)	Housner's model (Epstein, 1976)
Structural frequency (ω^2)	$\omega_n^2 = \frac{g}{R} \lambda_n \tanh(\lambda_n \frac{h}{R})$	$\omega^2 = \frac{g}{R} 1.84 \tanh(1.84 \frac{h}{R})$
The stiffness of the convective mass springs (k_c)	$k_{cn} = m_{cn} \frac{g}{R} \lambda_n \tanh(\lambda_n \frac{h}{R})$	$k_c = m_c \frac{g}{R} 1.84 \tanh \frac{1.84h}{R}$
Convective masses (m_{cn})	$m_{cn} = m_w \frac{2 \tanh(\lambda_n(h/R))}{\lambda_n(h/R)(\lambda_n^2 - 1)}$	$m_c = m_w \cdot 0.318 \frac{R}{h} \tanh(1.84(h/R))$
Impulsive mass (m_i)	$m_i = m_w \left(1 - \sum_{m=0}^{\infty} \frac{m_w}{m_w} \right)$	$m_i = m_w \frac{\tanh(1.74R/h)}{(1.74R/h)}$
Height of convective masses (h_{cn})	$h_{cn} = h \left[\frac{1}{2} - \frac{4}{\lambda_n(h/R)} \tanh(\lambda_n \frac{h}{2R}) \right]$	$h_c = \left[1 - \frac{\cosh(1.84h/R) - 1}{1.84h/R \sinh(1.84h/R)} \right] h$
Height of impulsive mass (h_i)	$h_i = h \left[\frac{1}{2} + \frac{1}{(m_i/m_w)} \sum_{m=0}^{\infty} \left(\frac{m_w}{m_w} \right) \left(\frac{h_m}{h} \right) \right]$	$h_i = 3/8h$

the convective mass; the mass of m_i consists of the impulsive mass of the fluid, the mass derived by the weight of container and by some parts of self-weight of the supporting structure (two-thirds of the supporting structure weight is recommended in ACI 371R and the total weight of the supporting structure is recommended by Priestley et al., 1986). This two-mass model suggested by Housner has been commonly used for seismic design of elevated tanks. The dynamic characteristics of this model are estimated by using the expressions given in Table 1. In this table, m_w is the total mass of the fluid and λ_n are the roots of the first-order Bessel function of the first kind ($\lambda_1 = 1.8112$; $\lambda_2 = 5.3314$; $\lambda_3 = 8.5363$). If one needs to consider additional higher modes of convective masses (m_{cn}), Bauer's expressions (Table 1) in which the mass centre of the fluid is referenced may be used.

Similar equivalent masses and heights for this model based on the work of Veletsos and co-workers (Malhotra et al., 2000), with certain modifications that make the procedure simple, are also suggested in the Eurocode-8 (EC-8). The recommended design values for the cylindrical ground-supported tanks in EC-8 are given in Table 2. In this table, C_i is the dimensionless coefficient, C_c is the coefficient dimension of ($s/m^{1/2}$), and h_i' and h_c' are the heights of the impulsive and convective masses, respectively, for the overturning moment.

After determination of the two masses of m_1 and m_2 , with their locations and stiffnesses of k_1 and k_2 , the necessary periods, base shear and overturning moment for design can be estimated using standard structural dynamic procedures.

3.2. Added mass approach

There are different ways to handle the fluid–structure interaction problems that can be investigated by the added mass approach (Westergaard, 1931; Barton and Parker, 1987; Doğangün et al., 1996a), the Eulerian approach

Table 2

Recommended design values for the first impulsive and convective modes of vibration as a function of the tank height-to-radius ratio (h/R) (Eurocode-8, 2003)

h/R	C_i	C_c	m_i/m_w	m_c/m_w	h_i/h	h_c/h	h'_i/h	h'_c/h
0.3	9.28	2.09	0.176	0.824	0.400	0.521	2.640	3.414
0.5	7.74	1.74	0.300	0.700	0.400	0.543	1.460	1.517
0.7	6.97	1.60	0.414	0.586	0.401	0.571	1.009	1.011
1.0	6.36	1.52	0.548	0.452	0.419	0.616	0.721	0.785
1.5	6.06	1.48	0.686	0.314	0.439	0.690	0.555	0.734
2.0	6.21	1.48	0.763	0.237	0.448	0.751	0.500	0.764
2.5	6.56	1.48	0.810	0.190	0.452	0.794	0.480	0.796
3.0	7.03	1.48	0.842	0.158	0.453	0.825	0.472	0.825

(Zienkiewicz and Bettles, 1978), the Lagrangian approach (Wilson and Khalvati, 1983; Olson and Bathe, 1983; Dogangun et al., 1996b, 1997; Dogangun and Livaoglu, 2004) or the Eulerian–Lagrangian approach (Donea et al., 1982) with the finite-element method. The simplest method of these is the added mass approach; while using the other approaches for analyses, special programs that include fluid elements or sophisticated formulations are necessary.

In the added mass approach, a mass that is obtained by different techniques is added to the mass of the structure at the fluid–structure interface. For a system subjected to an earthquake excitation, the general equation of motion can be written as

$$\mathbf{M}\ddot{\mathbf{u}} + \mathbf{C}\dot{\mathbf{u}} + \mathbf{K}\mathbf{u} = -\mathbf{M}\ddot{\mathbf{u}}_g, \quad (3)$$

where \mathbf{M} is the mass matrix, \mathbf{C} the damping matrix, \mathbf{K} the stiffness matrix, $\ddot{\mathbf{u}}_g$ the ground acceleration, \mathbf{u} the relative displacement and the overdots denote the derivatives of \mathbf{u} with respect to time. If the added mass approach is used, the regulating equation changes in the following form:

$$\mathbf{M}^*\ddot{\mathbf{u}} + \mathbf{C}\dot{\mathbf{u}} + \mathbf{K}\mathbf{u} = -\mathbf{M}^*\ddot{\mathbf{u}}_g, \quad (4)$$

where \mathbf{M}^* is the total mass matrix consisting of the structural mass matrix \mathbf{M} and added mass matrix (\mathbf{M}_a). In this approach, it is assumed that the added mass of \mathbf{M}_a synchronously vibrates with the structure; therefore, only the mass matrix is increased to consider the fluid effect, whereas stiffness and damping matrices do not change.

4. Approaches for soil–structure system

It has generally been recognized that the interaction between soil and structure can indeed affect the response of structures, especially for structures on relatively flexible soil. The inclusion of the soil–structure interaction effects is particularly important in the seismic analyses of structures located in active seismic zones. Therefore, accurate representation of the soil–structure interaction effects is a crucial part of the seismic analysis. Generally, a number of different sophisticated mathematical techniques and elaborate computer codes are available for assessing the effects of the soil–structure interaction for buildings and other liquid storage structures (Veletsos, 1984; Wolf, 1985; Youssef, 1998). Although the soil–structure interaction may be more important for elevated tanks due to most of the masses being lumped above the ground level and the foundation being supported on a relatively small area, few studies on this subject (Dieterman, 1988; Livaoglu, 2005; Livaoglu and Dogangun, 2005) have been carried out. The majority of the research devoted to estimate the behavior of the fluid and the supporting structure by using the fixed base assumption (Dutta et al., 2000a, b, 2001).

4.1. Simplified models

In the models discussed here (Fig. 4), the interaction problem for structure–soil systems is based on tanks on rigid foundation and homogeneous soil. Lateral and rocking vibrations are considered, because effects of these motions are generally more important than vertical and torsional vibrations, which are neglected in this study. The fluid–structure interactions are represented by the equivalent spring-mass system as proposed by Housner (1963), and soil–structure interactions are represented by equivalent springs, as suggested in FEMA 368/369 (2000).

In Fig. 4, k_y and k_θ represent the equivalent translational and rocking stiffness of the foundation that can be modelled with springs. These are attached to the central point of the rigid circular foundation. The stiffnesses of k_y and k_θ for

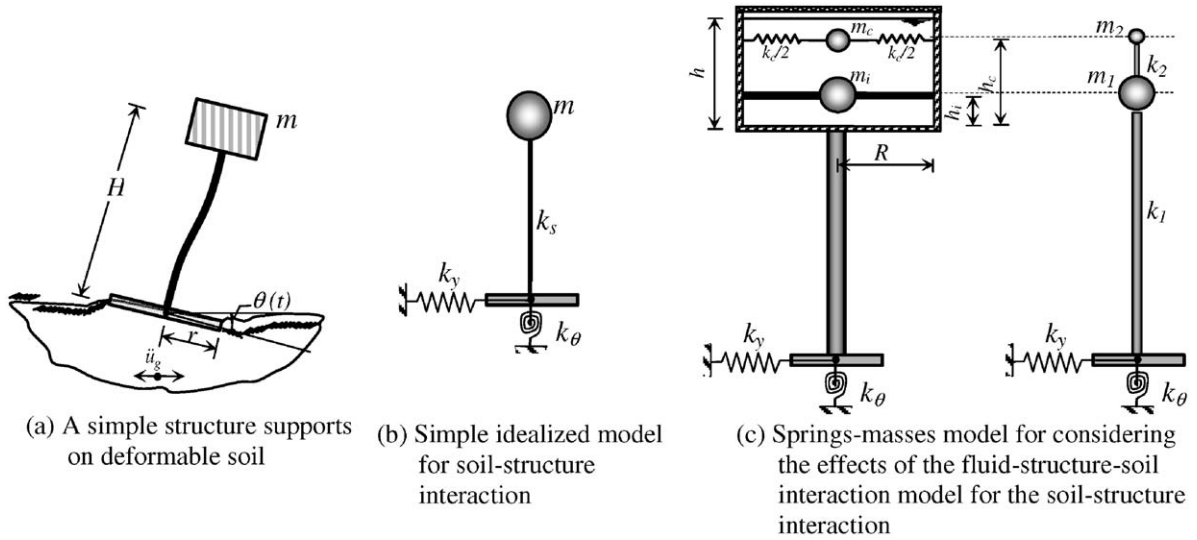


Fig. 4. Mechanical model for the fluid–structure–soil interaction of the elevated tank.

circular rigid foundations supported at the surface of a homogeneous halfspace are given by FEMA:

$$k_y = \left[\frac{8\alpha_y}{2 - \nu} \right] Gr, \quad k_\theta = \left[\frac{8\alpha_\theta}{3(1 - \nu)} \right] Gr^3, \tag{5}$$

where r is the radius of the foundation, G is the shear modulus of the halfspace, ν is the Poisson’s ratio for the soil, and α_y and α_θ are the dimensionless coefficients depending on the period of the excitation, the dimension of the foundation and the properties of the supporting medium. These stiffnesses are also estimated using the expressions given in FEMA for embedment and foundations that rest on a surface stratum of soil underlain by a stiffer deposit that has a shear-wave velocity more than twice that of the surface layer.

Veletsos et al. (1988) suggested a general expression for the effective damping ratio $\tilde{\xi}$ of the tank–foundation system; FEMA proposes a similar equation that can be written as

$$\tilde{\xi} = \xi_0 + \frac{\xi}{(\tilde{T}/T)^3}, \tag{6}$$

where ξ is the percentage of critical damping of the fixed-base elevated tank, ξ_0 is the contribution of the foundation damping, including the radiation (or geometric) damping and soil material damping, T is the natural period of the fixed-base elevated tank, and \tilde{T} is the modified period of the structure that verges on the flexibility of the supported system, and can be approximately estimated by

$$\tilde{T} = T \sqrt{1 + \frac{k}{k_y} \left(1 + \frac{k_y H^2}{k_\theta} \right)}, \tag{7}$$

where k is the equivalent stiffness and H is the height of the elevated tank.

As shown in Fig. 5, there are three important parameters that affect the value of ξ_0 : the first is the period ratio (\tilde{T}/T), the second is the height of the embedment of the foundation to the radius of the foundation (\hat{h}/r), and the last is the spectral response acceleration (S_D).

After the determination of the stiffness, the necessary parameters for design can be estimated by using the standard structural dynamic methods.

4.2. Massless foundation approach

Most structural analysis computer programs automatically apply the seismic loading to all mass degrees-of-freedom within the computer model and cannot solve the soil–structure interaction problem. This lack of capability has

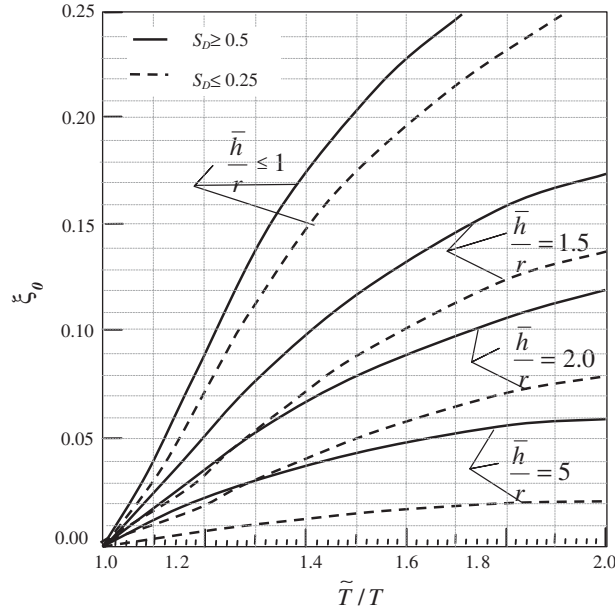


Fig. 5. Foundation damping factor (FEMA 368, 2000).

motivated the development of the massless foundation model (Wilson, 2002). This allows the correct seismic forces to be applied to the structure; however, the inertia forces within the foundation material are neglected. To activate the soil–structure interactions within general-purpose structural analysis programs, it is only necessary to identify the foundation mass in order that the loading is not applied to that part of the structure. In this study, the SAP2000 (2004) general-purpose structural analysis program has been selected not only to consider the soil/foundation–structure interaction but also the fluid–structure interaction for the elevated tanks.

The model considered for the massless foundation approach may be seen in Fig. 6. In this model, the soil/foundation–structure model is divided into three sets of node points. The common nodes at the interface of the structure and the foundation are identified with “c”; the other nodes within the structure are named “s”; and the other nodes within the foundation are “f” nodes. In this figure, the absolute displacement (U) is estimated from the sum of free-field displacement (v) and added displacement (u).

From the direct stiffness approach in structural analyses, the dynamic force equilibrium of the system is given in terms of the absolute displacements, U , by the following submatrix equation (Wilson, 2002):

$$\begin{bmatrix} M_{ss} & 0 & 0 \\ 0 & M_{cc} & 0 \\ 0 & 0 & M_{ff} \end{bmatrix} \begin{Bmatrix} \ddot{U}_s \\ \ddot{U}_c \\ \ddot{U}_f \end{Bmatrix} + \begin{bmatrix} K_{ss} & K_{sf} & 0 \\ K_{cf} & K_{cc} & K_{cf} \\ 0 & K_{fc} & K_{ff} \end{bmatrix} \begin{Bmatrix} U_s \\ U_c \\ U_f \end{Bmatrix} = \begin{Bmatrix} 0 \\ 0 \\ 0 \end{Bmatrix}, \quad (8)$$

where the mass and the stiffness at the contact nodes are the sum of the contribution from the structure (s) and foundation (f), and they are given by

$$M_{cc} = M_{cc}^{(s)} + M_{cc}^{(f)} \quad \text{and} \quad K_{cc} = K_{cc}^{(s)} + K_{cc}^{(f)}. \quad (9)$$

Three-dimensional free-field solutions are designated by absolute displacements v and the absolute accelerations \ddot{v} . By a simple change of variables, it is now possible to express the absolute displacements U and accelerations \ddot{U} in terms of displacements u relative to the free-field displacements v as given below:

$$\begin{Bmatrix} U_s \\ U_c \\ U_f \end{Bmatrix} \equiv \begin{Bmatrix} u_s \\ u_c \\ u_f \end{Bmatrix} + \begin{Bmatrix} v_s \\ v_c \\ v_f \end{Bmatrix} \quad \text{and} \quad \begin{Bmatrix} \ddot{U}_s \\ \ddot{U}_c \\ \ddot{U}_f \end{Bmatrix} \equiv \begin{Bmatrix} \ddot{u}_s \\ \ddot{u}_c \\ \ddot{u}_f \end{Bmatrix} + \begin{Bmatrix} \ddot{v}_s \\ \ddot{v}_c \\ \ddot{v}_f \end{Bmatrix} \quad (10)$$

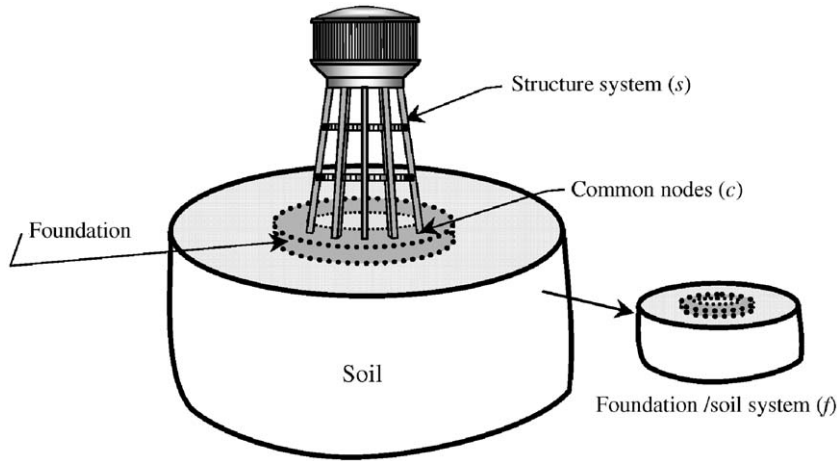


Fig. 6. Considered structure–foundation/soil interaction model.

Using Eqs. (9) and (10), Eq. (8) can now be written as

$$\begin{aligned}
 & \begin{bmatrix} M_{ss} & 0 & 0 \\ 0 & M_{cc} & 0 \\ 0 & 0 & M_{ff} \end{bmatrix} \begin{Bmatrix} \ddot{u}_s \\ \ddot{u}_c \\ \ddot{u}_f \end{Bmatrix} + \begin{bmatrix} K_{ss} & K_{sc} & 0 \\ K_{cs} & K_{cc} & K_{cf} \\ 0 & K_{fc} & K_{ff} \end{bmatrix} \begin{Bmatrix} u_s \\ u_c \\ u_f \end{Bmatrix} \\
 & = - \begin{bmatrix} M_{ss} & 0 & 0 \\ 0 & M_{cc} & 0 \\ 0 & 0 & M_{ff} \end{bmatrix} \begin{Bmatrix} \ddot{v}_s \\ \ddot{v}_c \\ \ddot{v}_f \end{Bmatrix} - \begin{bmatrix} K_{ss} & K_{sc} & 0 \\ K_{cs} & K_{cc} & K_{cf} \\ 0 & K_{fc} & K_{ff} \end{bmatrix} \begin{Bmatrix} v_s \\ v_c \\ v_f \end{Bmatrix} = \{R\}, \quad (11)
 \end{aligned}$$

where R is the load vector. Therefore, the right-hand side of Eq. (11) does not contain the mass of the foundation. Thus, the three-dimensional dynamic equilibrium equation with added damping for the complete soil–structure system is of the following form for a lumped-mass system:

$$M\ddot{u} + C\dot{u} + Ku = -m_x\ddot{v}_x - m_y\ddot{v}_y - m_z\ddot{v}_z. \quad (12)$$

The added, relative displacements, u , exist for the soil–structure system and must be set to zero at the sides and bottom of the foundation. The terms \ddot{v}_x , \ddot{v}_y and \ddot{v}_z are the free-field components of the acceleration if the structure is not present. The column matrices, m_x , m_y and m_z , are the directional masses for only the added structure.

5. Seismic analysis of a reinforced concrete elevated tank

A reinforced concrete elevated tank with a container capacity of 900 m³ is considered in seismic analysis (Fig. 7). The elevated tank has a frame supporting structure in which columns are connected by the circumferential beams at regular intervals, at 7 and 14 m height level. The tank container is of the Intze type. The container and the supporting structure have been used as a typical project in Turkey until recent years. Young's modulus and the weight of concrete per unit volume are taken to be 32 000 MPa and 25 kN/m³, respectively. The container is filled with water to a density of 1000 kg/m³.

The design of ground acceleration is taken to be 0.4g. So, it is assumed that elevated tanks are built in a high seismicity zone. Because the response modification coefficient is generally recommended to be around 2–3 for elevated tanks by the seismic codes (ACI371, EC-8 and FEMA), this factor is taken to be 2 for the analysis. This value is judgmental; larger values are assigned to systems with excellent energy dissipation capacity and stability, as ensured by specific design and detailing procedures (Rai, 2002). Because of the critical importance of this type of structure, the importance factor is taken to be 1.25 for the elevated tank.

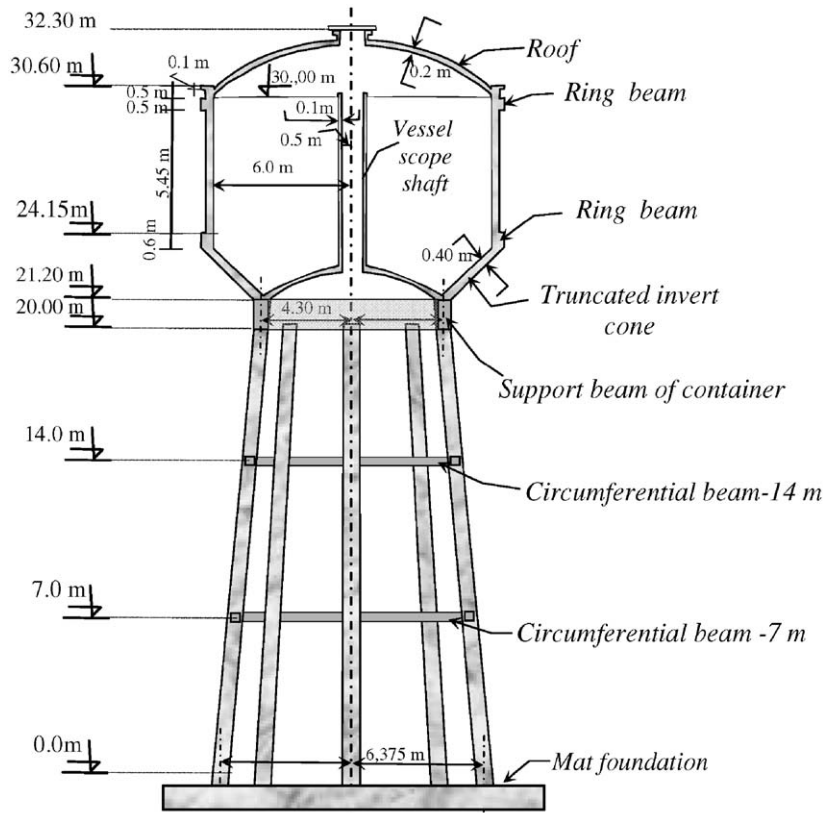


Fig. 7. Vertical cross-section of the reinforced concrete elevated tank considered for seismic analysis.

The analysis has been carried out considering four different subsoil classes as subgrade medium. The subsoil classes considered in this study can be classified as subsoil of classes A, B, D and E in EC-8. The soil properties considered for this paper are given in Table 3. The soil spring stiffnesses given in Table 3 have been calculated according to the expressions presented in Section 4.1.

The damping values for the reinforced concrete elevated tanks are taken as 5% for the impulsive mode and 0.5% for the convective mode, as recommended in most literature. The elastic response spectra drawn for the subsoil classes and for 5% and 0.5% damping can be seen in Fig. 8.

Seismic analyses for the selected elevated tanks are carried out under three main groups, as below:

- Single lumped-mass models
 - Fixed base assumption (Model 1)
 - Flexible soil assumption (Model 2)
- Models for considering fluid–structure interaction
 - Simplified models
 - Housner’s two-mass model (Model 3)
 - EC-8’s model (Model 4)
 - Finite-element models
 - Lumped-mass approximation (Model 5)
 - Westergaard’s Approximation
 - Housner’s expressions (Model 6)
 - EC-8’s expressions (Model 7)
- Models for considering fluid–structure–soil interaction
 - Mechanical model (Model 8)
 - Finite-element models
 - Subsoil modeled by springs (Model 9)
 - Subsoil modeled by finite element (Model 10)

Table 3

Properties of subsoil; shear wave velocity (v_s), unit weight of soil (γ), shear modulus (G), constraint modulus (E_c), Young's modulus (E), stiffnesses for subsoil (k_y and k_θ) and Poisson's ratio (ν)

Subsoil class	v_s (m/s)	γ (kN/m ³) (Coduto, 2001)	G (MPa)	E_c (MPa) (Bardet, 1997)	E (MPa)	k_y (kN/m)	k_θ (kN/m)	ν (Bardet, 1997)
A	1000	20	2,038,736	5,436,639	4,892,966	63,427,342	2,330,954,808	0.20
B	400	18	293,578	1,027,523	763,303	9,670,804	383,608,563	0.30
D	150	15	34,404	206,422	96,330	1,204,128	52,446,483	0.40
E	85	15	11,047	121,521	32,037	399,132	18,372,162	0.45

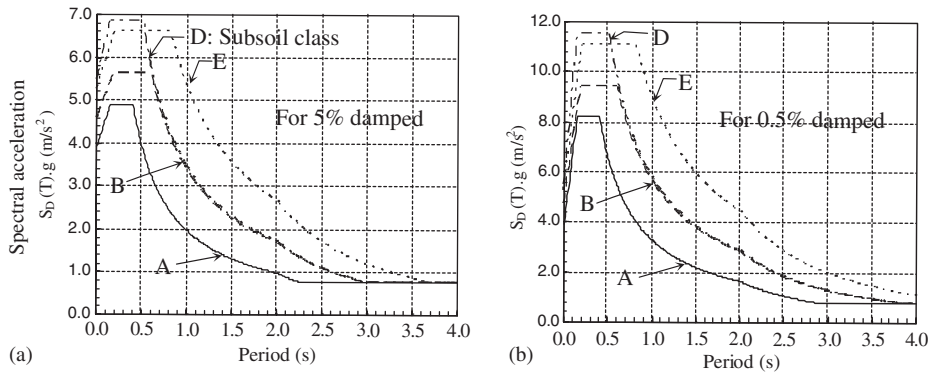


Fig. 8. Elastic response spectra of Type-1 recommended by Eurocode-8 for subsoil of classes A, B, D and E.

The ten models above are used for the three main groups shown. How the single-lumped mass model may be used for the elevated tank, and whether this model could represent the seismic behavior of the elevated tanks or not, are tested by Models 1 and 2 in this study. To account for the sloshing effects, the fluid–structure effect is taken into account and five different models (Models 3–7) are constructed. Simplified techniques are used for Models 3 and 4, and the finite-element model is used with simplified techniques for Models 5–7. Finally, Models 8–10 are established to take both soil and fluid interaction effects into account. Below, these three groups of models are used for investigating seismic analysis procedures.

5.1. Analysis using single lumped-mass model

Two groups of analyses, based on the fixed-base and flexible soil assumptions, were carried out for the single lumped-mass model (Models 1 and 2) of elevated tanks. The values of the stiffnesses and masses for these two analyses are shown in Fig. 9.

The fundamental period (T), base shear (V) and overturning moment (M_o) that was estimated for these two analyses are given in Table 4. The effective damping ratios, ξ , of the tank–foundation systems for four subsoil classes are estimated as 5%, 5%, 6.2% and 9.3% using Eq. (6).

As seen from Table 4, the results obtained for Models 1 and 2 are close to each other for the subsoil of class A. Smaller base shear and overturning moments are obtained for Model 2 in which the soil is assumed to be flexible. The difference between the period values for the subsoil class of E reaches 17% for both models. As seen later, these period values that were obtained for single-mass models are remarkably far from the impulsive period values.

5.2. Analysis considering fluid–structure interaction

Seismic analyses were carried out for five models that consider fixed-base assumptions. Analyses for Models 3 and 4 are carried out using simplified models that were recommended by Housner (1963) and EC-8 (2003). The other analyses

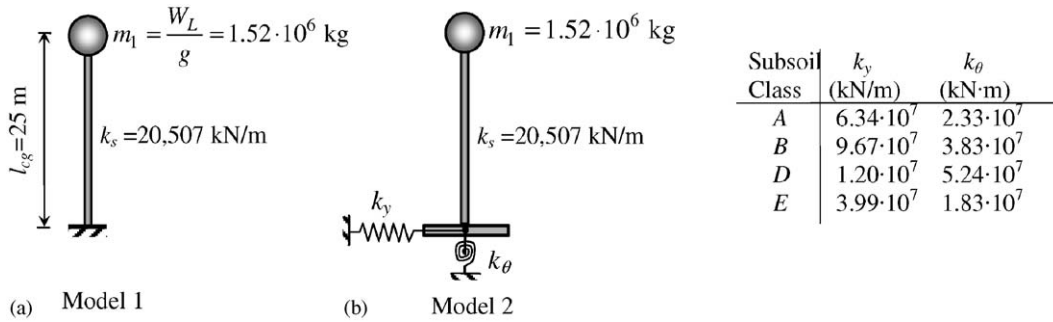


Fig. 9. The stiffness and mass values estimated for the single lumped-mass model of the elevated tank.

Table 4
Results obtained by the single lumped-mass models for two assumptions and four subsoil classes

Subsoil class	Fixed base assumption (Model 1)				Flexible soil assumption (Model 2)				% Deviation			
	A	B	D	E	A	B	D	E	A	B	D	E
T (s)	1.71	1.71	1.71	1.71	1.712	1.722	1.807	1.996	0	1	6	17
V (kN)	1742	2606	4697	3030	1189	2591	4121	2000	-32	-1	-12	-34
M_o (kNm)	43,556	65,145	117,412	75,750	29,724	64,766	103,020	49,995	-32	-1	-12	-34

for Models 5–7 were carried out using finite-element models with an added mass approach for fluid–structure interactions with the lumped-mass or distributed-mass techniques.

According to the EC-8 (2003) comments, if the container has a truncated inverted cone bottom, an equivalent cylinder may be considered, having the same volume of liquid as the real tank, and a diameter equal to that of the cone at the level of the fluid. Therefore, an equivalent cylinder is considered for the estimations of equivalent masses and stiffnesses for fluid. The values of the stiffnesses and masses for the simplified models given in Fig. 10 are estimated using the expressions recommended by Housner (1963) and EC-8 (2003). The lateral stiffness of the supporting structure (k_l) given in Fig. 10 is estimated using the finite-element method. This stiffness is also calculated with the equation below that is given for this type of supporting structure by Dutta et al. (2000b):

$$k_l = \frac{12E_{cl}I_{cl}N_{cl}}{h_{cl}^3} \left[\frac{1}{\frac{2I_{cl}N_p(4N_p^2-1)}{A_e R_s^2} + N_p + 2(N_p - 1) \frac{E_{cl}I_{cl}/h_{cl}}{E_b I_b/L}} \right] \rightarrow k_l = 31\,904 \text{ kN/m.}$$

In the equation above, E_{cl} , h_{cl} , I_{cl} and N_{cl} are Young’s modulus of the column material, the net height, the moment of inertia and the number of the columns, respectively; E_b , L and I_b are Young’s modulus of the beam material, span and moment of inertia of the beam, respectively; N_p is the number of panels and R_s is the staging radius.

The finite-element mesh, as shown in Fig. 11, is generated and is intended to model the influence of fluid–structure effects on the seismic behavior of elevated tanks. Degrees-of-freedom at the base nodes are fixed and at the other nodes are left free for the system, which is the well-known fixed-base system. Columns and beams are modelled with the frame element; walls and truncated cones of the container are modelled with the shell element. The added mass approach is selected for the fluid–tank interaction using the finite-element method. For impulsive mass, Westergaard’s approximation, which may be called the distributed-added-mass approach, is used. Convective mass is lumped at the center and at a height h_c of the container. This mass is connected to the joints of the finite element at the same height level as the spring, the total stiffness value of which, for one direction, is k_c . The contribution of this mass to the dynamic behavior of elevated tanks for the vertical direction is also considered.

Impulsive mass, which is obtained for the fluid, may be added to the mass of the container with different techniques. Three techniques are used in this paper. In the first technique, as can be seen in Fig. 11(a), lumped impulsive mass obtained by EC-8 is equally added to the mass of the finite element of container walls from the bottom to the height of $[h_i + (h_i - h_c)/2]$. In the second and third techniques, as shown in Figs. 11(b) and (c), the hydrodynamic pressure distribution acting on container walls is estimated according to values given by Housner and EC-8, respectively. Then,

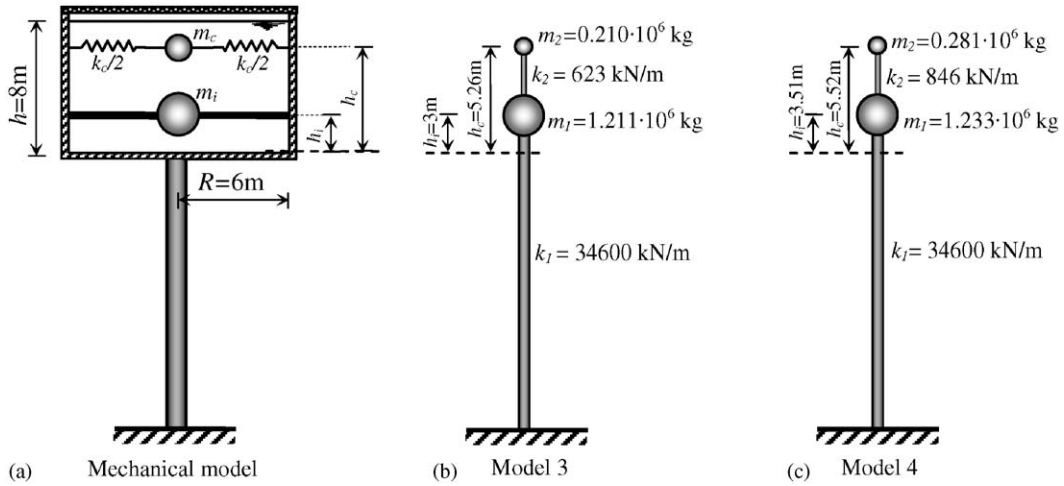


Fig. 10. The stiffness and mass values estimated for the two-mass model of Housner and Eurocode-8 with the assumption of fixed-base.

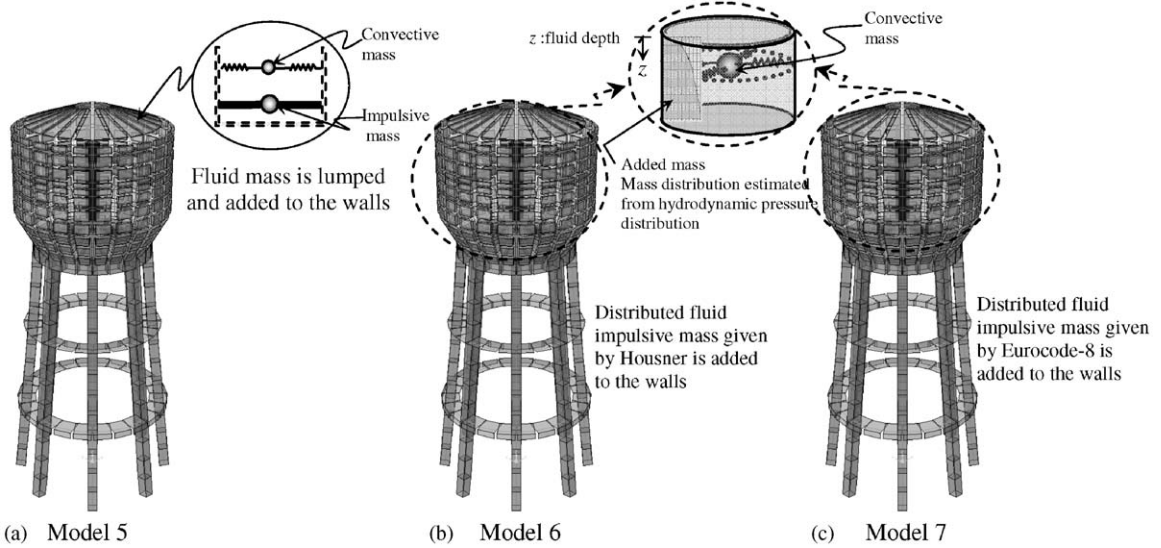


Fig. 11. Finite element mesh of the fluid–structure system for the added mass approach with the assumption of the fixed-base.

the mass distribution is determined in accordance with the hydrodynamic pressure distribution. This approach is based on Westergaard’s added mass approach that was developed for dams. It should be noted here that, as the total mass is different from the sum of the impulsive and convective masses in the Housner model, the residual mass should be added to the bottom structural elements of the container.

The periods for the sloshing mode (T_c), and for the impulsive mode (T_i), the base shears (V) and the overturning moments (M_o), are given in Table 5 for the simplified models; Tables 6 and 7 show the finite-element models that appeared in Fig. 11. Tables 6 and 7 also include the maximum lateral displacements (δ_{max}) of the elevated tank.

Instead of illustrating comparisons, the values obtained from the results of the analyses are exhibited in tables. All comparisons for models used to investigate fluid–structure interactions are coincident with the figures. As can be seen from Tables 5–7, the period values are close to each other for five models. The maximum difference for the overturning moments is 4% for the lumped-mass (Model 5) and the distributed added mass (Model 7) approximation. Models 6 and 7, in which the distributed added mass used may be recommended for design, show how the fixed-base-assumption is used. If the masses are not added at the actual height, the overturning moment may be underestimated. This is because the maximum difference can only reach approximately 1% of the added mass approximations using distributed masses

Table 5

Results obtained for four subsoil classes by the two-mass models (Models 3 and 4) recommended by Housner and Eurocode-8 for considering fluid–structure interaction

Subsoil class	Housner's model (Model 3)				Eurocode-8's model (Model 4)				% Deviation			
	A	B	D	E	A	B	D	E	A	B	D	E
T_c (s)	3.690	3.69	3.690	3.690	3.674	3.674	3.674	3.674	−0.43	−0.43	−0.43	−0.43
T_i (s)	1.166	1.16	1.166	1.166	1.172	1.172	1.172	1.172	0.51	0.51	0.51	0.51
V (kN)	2439	3670	6594	4273	2471	3688	6625	4291	1.33	0.49	0.48	0.47
M_o (kNm)	64,730	97,425	175,080	113,424	66,003	98,213	176,406	114,269	1.97	0.81	0.76	0.75

Table 6

Results obtained for four subsoil classes by the finite element models (Models 5 and 7) with the lumped and added mass approaches for considering the fluid–structure interaction

Subsoil class	Lumped-mass approximation using equivalent masses given in Eurocode-8 (Model 5)				Added mass approximation using distributed masses given in Eurocode-8 (Model 7)				% Deviation			
	A	B	D	E	A	B	D	E	A	B	D	E
T_c (s)	3.668	3.668	3.668	3.668	3.663	3.663	3.663	3.663	−0.13	−0.13	−0.13	−0.13
T_i (s)	1.061	1.061	1.061	1.061	1.036	1.036	1.036	1.036	−2.35	−2.35	−2.35	−2.35
V (kN)	2716	4052	4651	4723	2706	4038	4635	4708	−0.3	−0.3	−0.3	−0.3
M_o (kNm)	60,850	90,501	103,777	105,455	63,370	94,393	108,276	110,022	4.1	4.2	4.9	4.3
δ_{\max} (mm)	59	88	101	102	58	86	99	101	−1.7	−2.2	−1.9	−0.9

Table 7

Results obtained for four subsoil classes by the finite element models (Models 6 and 7) with Westergaard's added mass approach for considering the fluid–structure interaction

Subsoil class	Added mass approximation using distributed masses proposed by Housner (Model 6)				Added mass approximation using distributed masses given in Eurocode-8 (Model 7)				% Deviation			
	A	B	D	E	A	B	D	E	A	B	D	E
T_c (s)	3.680	3.680	3.680	3.680	3.663	3.663	3.663	3.663	−0.46			
T_i (s)	1.035	1.035	1.035	1.035	1.036	1.036	1.036	1.036	−0.03	−0.03	−0.03	−0.03
V (kN)	2731	4081	4686	4760	2706	4038	4635	4708	−0.9	−1.1	−1.1	−1.1
M_o (kNm)	63,813	95,244	109,297	111,061	63,370	94,393	108,276	110,022	−0.7	−0.9	−0.9	−0.9
δ_{\max} (mm)	58	87	100	102	58	86	99	101	0.0	−1.3	−1.0	−1.0

estimated by the expressions given by Housner (Model 6) and EC-8 (Model 7). Both approximations can similarly be used. Also, a 4% deviation is considered an allowable difference. Therefore, it can be stated that the lumped-mass assumption for Model 5 is an adequate method to use with the simplified models.

5.3. Analysis considering fluid–structure–soil interaction

Seismic analyses for Models 8–10, as shown in Fig. 12(a)–(c), are carried out in this section. In the finite-element models, the added mass approach is used for considering fluid–structure interactions. The substructure approach for

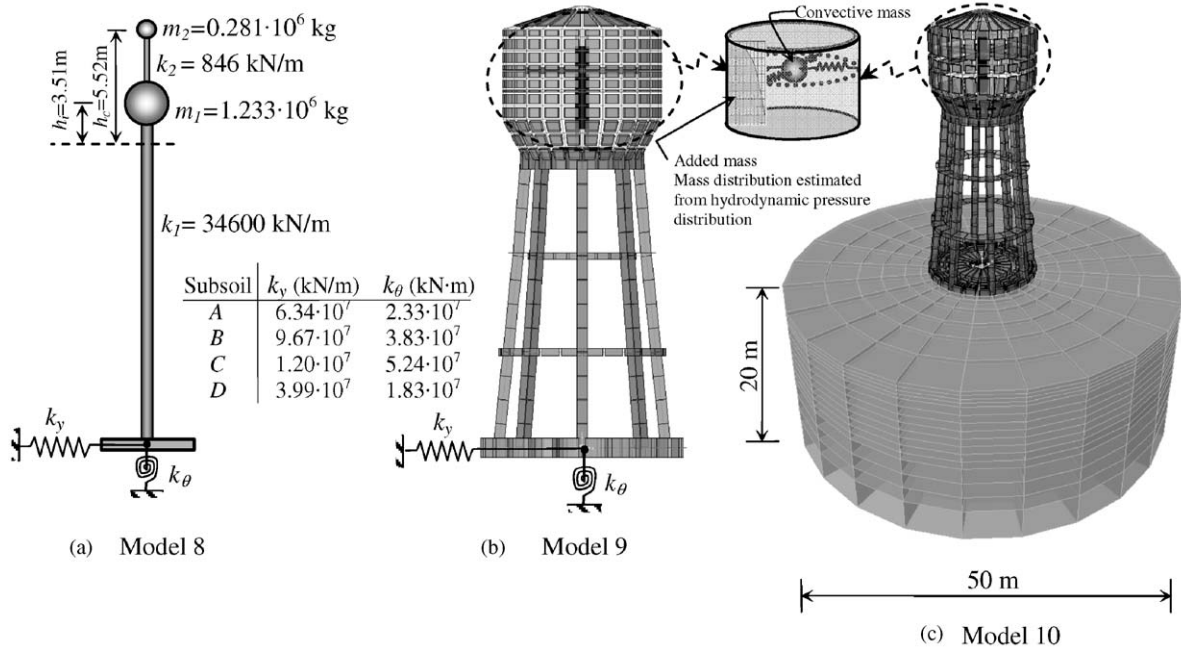


Fig. 12. Selected mechanical model and the finite element models for the soil–structure–fluid system.

Table 8

Results obtained by a mechanical model (Model 8) and the finite element models using the finite element for subsoil (Model 10)

Subsoil class	Mechanical model using equivalent stiffnesses and masses (Model 8)				Finite element models using finite element for subsoil (Model 10)				% Deviation			
	A	B	D	E	A	B	D	E	A	B	D	E
T_c (s)	3.674	3.675	3.675	3.677	3.66	3.67	3.69	3.74	0.3	0.1	−0.4	1.7
T_i (s)	1.172	1.173	1.179	1.192	1.04	1.07	1.25	1.57	−11	−9	6	32
V (kN)	3433	5297	2920	1941	2696	3958	2871	1570	−21	−25	−2	−19
M_o (kNm)	91,415	14,1041	77,772	51,848	63,149	92,837	67,981	37,027	−31	−34	−13	−29

Models 8 and 9 (Fig. 12(a) and (b)) and the massless foundation approach for Model 10 (Fig. 12(c)) are used to consider the soil–structure interactions. Three-dimensional finite-element meshes (shown in Fig. 12(b) and (c)) are generated and intended to model the influence of the fluid–structure and soil–structure effects on the seismic behavior of elevated tanks. A parametric study is carried out to estimate the distances of the soil boundaries. The subsoil beyond these boundaries does not affect the seismic behavior of the tank. In other words, when the system is analysed, the displacements at the nodes on the lateral boundaries are almost zero. The common nodes on the interface of the structure and foundation are free, but the soil nodes on the bottom boundaries are fixed. Due to a lack of rotational freedom capability of the brick element on the surface of the soil–structure interaction, the foundation is modelled with the shell element. The subsoil is modelled with an isoparametric-8 node-brick element that has three translational degrees of freedom per node.

The periods for sloshing mode (T_c), for impulsive mode (T_i), the base shear (V), the overturning moment (M_o) and their deviations are given in Table 8 for Model 8 using the equivalent stiffnesses and masses and the finite-element model (Model 10) using the finite element for the subsoil. Also, in Table 9, in addition to the parameters above, the column maximum axial forces (N_{\max}) and the maximum lateral displacement (δ_{\max}) obtained by the finite-element models as shown in Fig. 12(b) and (c) are given.

Table 9

Results obtained by finite element models using equivalent stiffnesses for soil (Model 9) and the finite element models using the finite element for subsoil (Model 10)

Subsoil class	Finite element models using equivalent stiffnesses for soil (Model 9)				Finite element models using finite element for soil (Model 10)				% Deviation			
	A	B	D	E	A	B	D	E	A	B	D	E
T_c (s)	3.66	3.67	3.69	3.75	3.66	3.67	3.69	3.74	0	0	-0.1	-0.2
T_i (s)	1.04	1.07	1.26	1.60	1.04	1.07	1.25	1.57	0	0	-0.8	-1.8
V (kN)	2695	3918	3720	2824	2696	3958	2871	1570	0	1.0	-23	-44
M_o (kNm)	63,127	91,836	88,494	67,451	63,149	92,837	67,981	37,027	0	1.1	-23	-45
N_{max} (kN)	2102	3055	2959	2273	2102	3085	2278	1264	0	1.0	-23	-44
δ_{max} (mm)	59	91	134	178	59	91	100	160	0	0	-25	-10

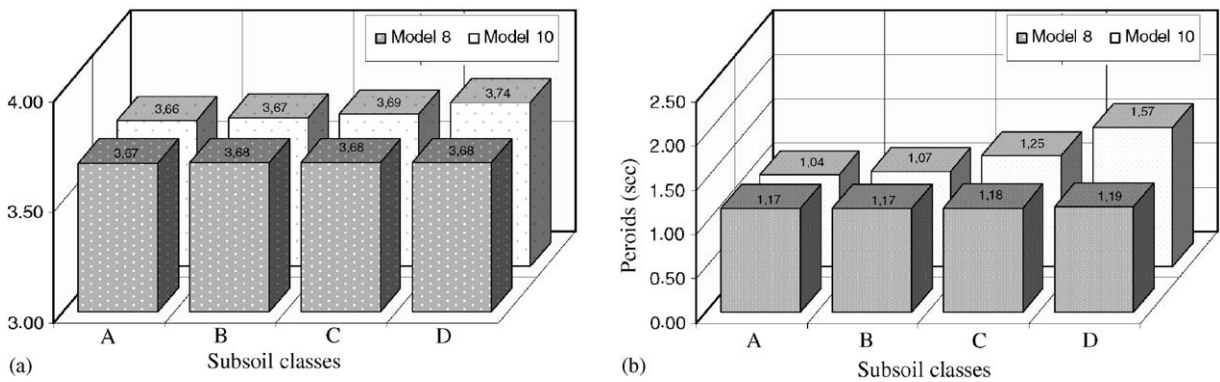


Fig. 13. Comparisons of the periods of (a) the convective mode and (b) impulsive mode for Models 8 and 10 according to subsoil class.

The variations of the impulsive mode in relation to the subsoil classes in Fig. 13(a) shows that the larger value is obtained for the D soil class. Another conspicuous result in Fig. 13(a) is that the values of the impulsive mode period increase for subsoil classes A–E from 1.172 to 1.192 s in the simplified model (Model 8), and from 1.04 to 1.57 s for the finite-element model (Model 10). It can be stated according to the deviation that if the soil gets softer, the period of the impulsive mode increases. However, the convective mode periods are not remarkably different, depending on the subsoil class (Fig. 13(b)).

As can be seen from Fig. 14, Model 8 gives a larger base shear than those obtained from the finite-element models (Models 9 and 10). Although internal forces decrease after subsoil class B, lateral displacements gradually increase depending on the softness of the soil (Fig. 15)—that is, lateral displacements are increased from 59 to 178 mm between the subsoil classes of A and D and it can be seen that this increase reaches 201% between subsoil classes A and D for Model 9, but for Model 10 this drops to 171%.

5.4. General comparisons of results

A total of 40 seismic analyses were carried out and all values were obtained for these analyses and given in tabulated form, so few comparisons are made in this section for the sake of brevity.

The periods for the impulsive and convective modes are illustrated for subsoil class of A for all ten models in Fig. 16(a) and (b), respectively, and also for the base shears in Fig. 17(a) and (b). As can be seen from Fig. 16(a), due to the lack of the sloshing mass, single lumped-mass models (Models 1 and 2) give relatively large period values. The other models give values that are close to each other for the impulsive mode. It is shown in Fig. 16(b) that almost all models

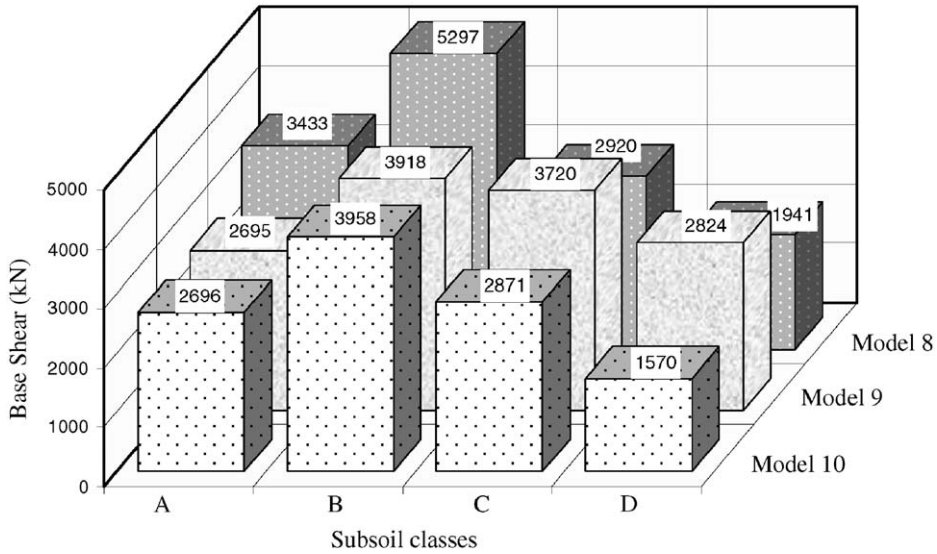


Fig. 14. Comparisons of the base shear forces for Models 8–10 according to subsoil class.

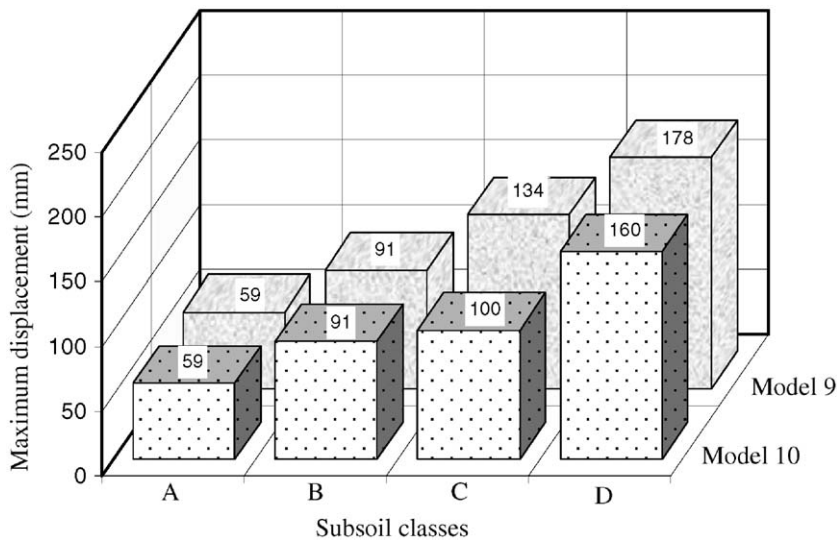


Fig. 15. Comparisons of the displacements for Models 9 and 10 according to subsoil class.

give similar period values for the convective mode. Because the convective mode is not considered for the single lumped-mass models, they are not shown in the figure.

As seen in Fig. 17(a), the maximum base shear is obtained for Model 8 for elevated tanks on subsoil of class A, and class D gives the lowest values. In Models 9 and 10, the equivalent stiffnesses and masses are used for the fluid. If Fig. 17(a) and (b) are compared with each other, it is seen that soil–structure interactions play effective roles in the decrease of the base shear forces. In other words, because the soil–structure interaction effects are ignored in the models (such as Models 1–7), the base shears are larger than in Models 8–10. It is shown in Fig. 17(a) that single lumped-mass models give underestimated base shear values. As overturning moments exhibit similar trends in base shear according to the models, figures are not shown for this.

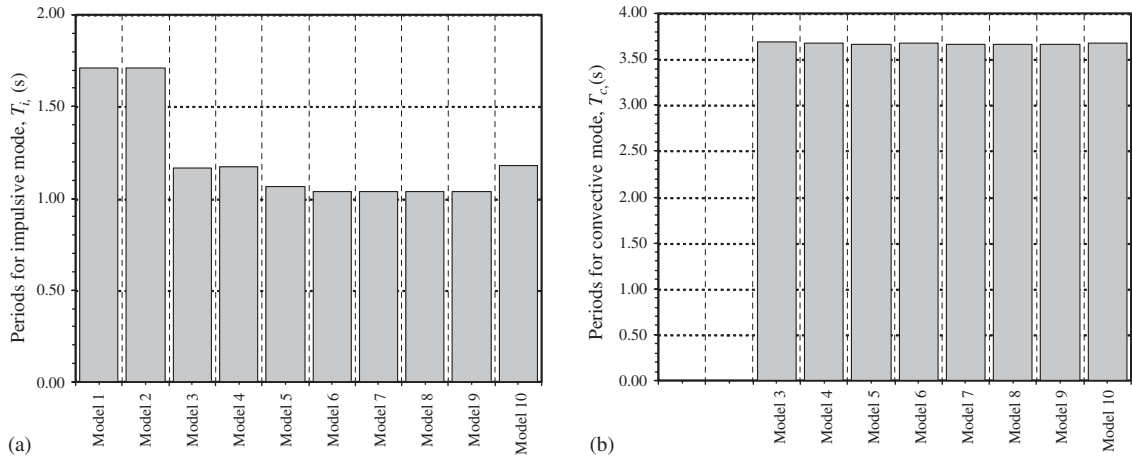


Fig. 16. Periods for (a) impulsive mode and (b) convective mode obtained for ten models considered for subsoil of class A.

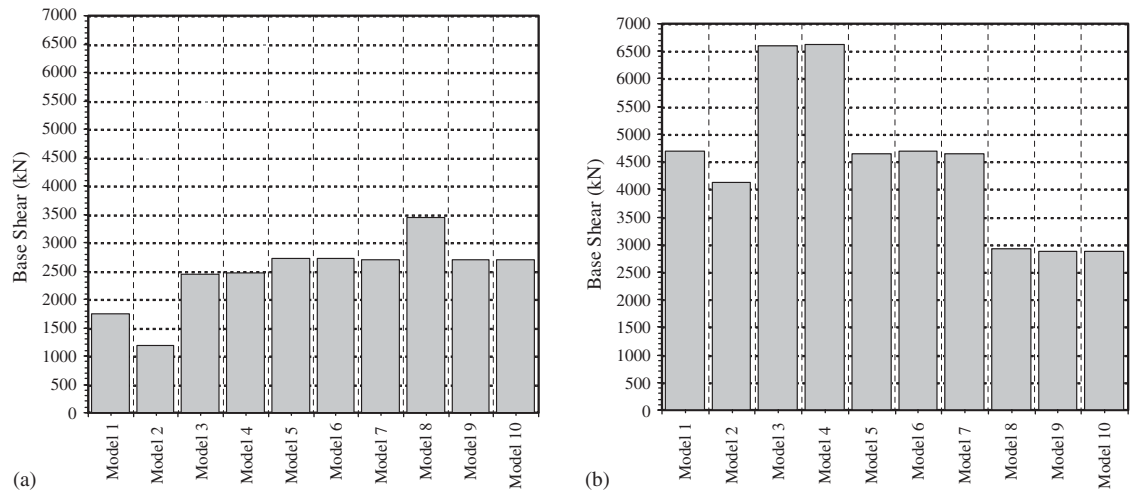


Fig. 17. Base shears obtained for ten models considered for subsoil of (a) class A and (b) class D.

6. Conclusions

The seismic design of elevated tanks by using single lumped-mass models provides smaller base shears and overturning moment in both fixed-base and flexible soil conditions. These circumstances may lead to unsafe seismic design of R/C elevated tanks. The period values were estimated to be near to 2 s for these models. These period values are far from the impulsive mode periods of around 1.1 s that have been estimated from the other models in which sloshing is considered. However, the impulsive mode of vibration strongly dominates the seismic behavior of elevated tanks.

Periods for convective modes are not remarkably different according to the soil–structure interactions of elevated tanks. In other words, similar period values are obtained for all models that are considered here. The maximum difference is generally under 0.5%.

The seismic design of the R/C elevated tanks, based on the rough assumption that the subsoil is rigid or rock without any site investigation, may lead to a wrong assessment of the seismic base shear and overturning moment. Three or more times larger base shears may be obtained, especially for subsoil of class D. Generally, small base shear and overturning moments are obtained for soft soils. Sometimes, lateral displacements are ignored in the design. However, they may reach three or more times larger values and these large displacements lead to instability of the elevated tank.

The added mass approach has the advantage of not using any fluid finite element. It may be recommended that the distributed added mass approach for seismic analysis of elevated tanks be used in general-purpose structural analyses programs. It should be noted that the lumped mass approach may lead to underestimations of the base shear and the overturning moment.

For the finite-element models in which the fluid–structure–soil interactions are considered, remarkably different base shears, overturning moments, axial forces and lateral displacement are obtained for soft soil conditions (subsoil classes of D and E). Therefore, for soft soil conditions, it is necessary to verify the results obtained by the practical methods given in this paper, which provide analyses without any special fluid and soil elements.

References

- ACI 371R-98 (American Concrete Institute), 1995. Guide to the Analysis Design and Construction of Concrete-pedestal Water Tower. ACI 371R.
- ADINA, 2004. Automatic Dynamic Incremental Nonlinear Analysis. ADINA R & D, Inc, Watertown, MA 02472, USA.
- ANSYS, 2004. Inc. Southpointe, 275 Technology Drive. Canonsburg, PA 15317, USA.
- Bardet, P.J., 1997. Experimental Soil Mechanics. Prentice-Hall, Upper Saddle River, NJ.
- Barton, D.C., Parker, J.V., 1987. Finite element analysis of the seismic response of anchored and unanchored liquid storage tanks. *Earthquake Engineering and Structural Dynamics* 15, 299–322.
- Bauer, H.F., 1964. Fluid oscillations in the containers of a space vehicle and their influence upon stability. NASA TR R 187.
- Chandrasekaran, A.R., Krishna, J., 1954. Water towers in seismic zones. In: Proceedings of the Third World Conference on Earthquake Engineering, New Zealand, vol. IV, pp. 161–171.
- Chavez, J.W., Fenves, G.L., 1994. EAGD-SLIDE: a computer program for the earthquake analysis of concrete gravity dams including base sliding. Structural Engineering, Mechanics, and Materials, Department of Civil and Environmental Engineering, Report No. UCB/SEMM-94/02, University of California, Berkeley, USA.
- Chen, C.P., Barber, R.B., 1976. Seismic design of liquid storage tanks to earthquakes. International Symposium on Earthquake Structural Engineering, St. Louis, MO, vol. II, pp. 1231–1247.
- Coduto, P.D., 2001. Foundation Design: Principles and Practices, second ed. Prentice-Hall, Upper Saddle River, NJ.
- Dieterman, H.A., 1988. Dynamics of tower, liquid–structure–foundation interaction. Ph.D. Dissertation, TU Delft, Netherlands.
- Doğangün, A., Durmus, A., Ayvaz, Y., 1996a. Finite element analysis of seismic response of rectangular tanks using added mass and Lagrangian approach. Proceedings of the Second International Conference on Civil Engineering Computer Applications Research and Practice, Bahrain, April 6–8, vol. I, pp. 371–379.
- Doğangün, A., Livaoglu, R., 2004. Hydrodynamic pressures acting on the walls of rectangular fluid containers, *Structural Engineering and Mechanics* 17, 203–214.
- Doğangün, A., Durmus, A., Ayvaz, Y., 1996b. Static and dynamic analysis of rectangular tanks by using the Lagrangian fluid finite element. *Computers & Structures* 59, 547–552.
- Doğangün, A., Durmus, A., Ayvaz, Y., 1997. Earthquake analysis of flexible rectangular tanks using the Lagrangian fluid finite element. *European Journal of Mechanics-A/Solids* 16, 165–182.
- Donea, J., Guliani, S., Halleux, J.P., 1982. An arbitrary Lagrangian–Eulerian Finite Element method for transient dynamic fluid–structure interaction. *Computer Methods in Applied Mechanics and Engineering* 33, 689–723.
- Dutta, S.C., Jain, S.K., Murty, C.V.R., 2000a. Alternate tank staging configurations with reduced torsional vulnerability. *Soil Dynamics and Earthquake Engineering* 19, 199–215.
- Dutta, S.C., Jain, S.K., Murty, C.V.R., 2000b. Assessing the seismic torsional vulnerability of elevated tanks with RC frame-type staging. *Soil Dynamics and Earthquake Engineering* 19, 183–197.
- Dutta, S.C., Jain, S.K., Murty, C.V.R., 2001. Inelastic seismic torsional behavior of elevated tanks. *Journal of Sound and Vibration* 242 (1), 151–167.
- Epstein, H.I., 1976. Seismic design of liquid-storage tanks. *ASCE Journal of Structural Division* 102, 1659–1673.
- Eurocode-8, 2003. Design of structures for earthquake resistance—Part 1. 1:General rules—Seismic action and general requirements for structures—Part 4: Silos, tanks and pipelines. European Committee for Standardization, Final PT Draft.
- FEMA 368/369, 2000. The 2000 NEHRP Recommended Provisions for New Buildings and Other Structures, Part 1: Provision and Part 2: Commentary. Federal Emergency Management Agency, Washington.
- Fischer, F.D., Rammerstorfer, F.G., Scharf, K., 1991. Earthquake resistant design of anchored and unanchored liquid storage tanks under three dimensional earthquake excitation. In: Schueller, G.I. (Ed.), *Structural Dynamics—Recent Advances*. Springer, Amsterdam, pp. 317–371.
- Haroun, M.A., Housner, G.W., 1981. Seismic design of liquid storage tanks. *ASCE Journal of Technical Councils* 107 (1), 191–207.
- Haroun, M.A., Ellaithy, M.H., 1985. Seismically induced fluid forces on elevated tanks. *Journal of Technical Topics in Civil Engineering* 111, 1–15.
- Housner, G.W., 1963. Dynamic behavior of water tanks. *Bulletin of the Seismological Society of the America* 53, 381–387.

- Livaoglu, R., 2005. Investigation of the earthquake behavior of elevated tanks considering fluid–structure–soil interactions. Ph.D. Thesis, Karadeniz Technical University, Trabzon, 2005 (in Turkish).
- Livaoglu, R., Doğangün, A., 2005. Sismic evaluation of fluid-elevated tank-foundation/soil systems in frequency domain. *Structural Engineering and Mechanics* 21, 101–119.
- Malhotra, P.K., Wenk, T., Weiland, M., 2000. Simple procedure of seismic analysis of liquid-storage tanks. *Journal of Structural Engineering International, IABSE* 10 (3), 197–201.
- Olson, L.G., Bathe, K.J., 1983. A study of displacement-based fluid finite elements for calculating frequencies of fluid and fluid–structure systems. *Nuclear Engineering and Design* 76, 137–151.
- Priestley, M.J.N., Davidson, B.J., Honey, G.D., Hopkins, D.C., Martin, R.J., Ramsey, G., Vessey, J.V., Wood, J.H., 1986. *Seismic Design of Storage Tanks. Recommendation of a study group the New Zealand Society for Earthquake Engineering, New Zealand.*
- Rai, D.C., 2002. Seismic retrofitting of R/C shaft support of elevated tanks. *Earthquake Spectra* 18, 745–760.
- SAP2000, 2004. *Integrated Software for Structural Analysis & Design.* Computers and Structures Inc., Berkeley, CA.
- SOLVIA, 2004. *The Finite Element System for Linear and Nonlinear Analysis of Displacements, Stresses and Temperatures Under Static or Dynamic Conditions.* SOLVIA Engineering AB, Sweden.
- Tan, H., Chopra, A.K., 1996. EACD-3D-96—Three-dimensional Earthquake Analysis of Concrete Dams. Department of Civil and Environmental Engineering, University of California, Berkeley, USA.
- Veletsos, A.S., 1984. *Seismic Response and Design of Liquid Storage Tanks, Guidelines for the Seismic Design of Oil and Gas Pipeline Systems.* ASCE, New York, pp. 255–461.
- Veletsos, S.A., Prasad, M.A., Tang, Y., 1988. Design approaches for soil structure interaction. Technical Report NCEER-88-00331, National Center for Earthquake Engineering Research.
- Westergaard, H.M., 1931. Water pressures on dams during earthquakes. *Proceedings of the ASCE* 57, 1303.
- Wilson, E.L., 2002. *Three-dimensional Static and Dynamic Analysis of Structures—a Physical Approach with Emphasis on Earthquake Engineering*, third ed. Computers and Structures Inc, Berkeley, CA, USA.
- Wilson, E.L., Khalvati, M., 1983. Finite elements for the dynamic analysis of fluid-solid systems. *International Journal of Numerical Methods in Engineering* 19, 1657–1668.
- Wolf, J.P., 1985. *Dynamic Soil–Structure Interaction.* Prentice-Hall, Englewood Cliffs, NJ.
- Youssef, A., 1998. Seismic response of inelastic structures on compliant foundations. Ph.D. Dissertation, Department of Civil and Environmental Engineering, Northeastern University Boston, MA, USA.
- Zeiny, A., 1995. Nonlinear time-dependent seismic response of unanchored liquid storage tanks. Ph.D. Dissertation, University of California, Irvine, CA, USA.
- Zienkiewicz, O.C., Bettles, P., 1978. Fluid-structure dynamic interaction and wave forces; an introduction to numerical treatment. *International Journal of Numerical Methods in Engineering* 13, 1–16.